PHYSICAL REVIEW B **71**, 201402(R) (2005)

Second-harmonic generation from nanoscopic metal tips: Symmetry selection rules for single asymmetric nanostructures

Catalin C. Neacsu,[1] Georg A. Reider,[2] and Markus B. Raschke[1]
[1]*Max-Born-Institut für Nichtlineare Optik und Kurzzeitspektroskopie, D-12489 Berlin, Germany*
[2]*Institut für Photonik, Technische Universität Wien, A-1040 Wien, Austria*
(Received 18 April 2005; published 31 May 2005)

Second-harmonic generation (SHG) from individual nanoscopic metal tips has been investigated. Compared to both planar interfaces, as well as spherical or ellipsoidal nanoparticles, very different polarization selection rules and SH-emission directions result. As a partially asymmetric nanostructure the tip allows for the distinction of otherwise inseparable local surface and nonlocal bulk second-harmonic polarizations. This provides opportunities for second-harmonic investigations of nanoparticles and in scattering-type near field microscopy.

DOI: 10.1103/PhysRevB.71.201402 PACS number(s): 78.67.−n, 42.65.An, 42.65.Ky, 78.68.+m

The optics of media of dimensions small compared to the optical wavelength is characterized by distinctive phenomena such as optical field confinement and structural resonances. With a strong focus in research on the linear optical processes of surface nanostructures and colloids, the nonlinear optical properties have remained largely unexplored. The nonlinear response, however, is expected to differ fundamentally due to its high symmetry selectivity. Specifically, for media with inversion symmetry the second-order nonlinearity is dominated by the interface where the symmetry is broken.[1] Second-harmonic generation (SHG) has thus become a well-established technique for the investigation of planar surfaces and interfaces.[2] Many applications, however, would call for an expansion of SHG to also address molecular adsorption and surface electronic and geometric structure on the nanoscale. Here, the problem of SHG becomes particularly intriguing: Although at the surface of the nanostructure the inversion symmetry is broken locally, depending on its dimension and macroscopic symmetry, emission can be highly restricted due to the destructive interference of the induced local surface second-harmonic (SH) polarizations.[3,4]

In this paper we address the different contributions to the nonlinear source polarization and provide general directional and polarization selection rules for second-harmonic generation from partially asymmetric (*mm*) nanostructures. Metal wire tips with a nanometer-sized apex represent a model geometry, with the mirror symmetry being broken along the tip axis but conserved in all other directions. This structure allows for the direct separation between local surface and nonlocal higher-order bulk contributions to the SH response—a long-standing problem in nonlinear surface spectroscopy.[1,5] Recently, an attempt to resolve this issue for nanoparticles has been made,[6] yet the separation of surface and bulk contributions remained open.

In SHG strong symmetry selection rules apply that are valid independent of the microscopic origin of the nonlinear polarization.[5,7] For media with inversion symmetry the process of SHG (and any other even-order nonlinear process) is forbidden in the electric dipole approximation. In contrast, the broken mirror symmetry at the interface allows for a local, second-order source polarization $\mathbf{P}^{(2)}(2\omega) = \epsilon_0 \boldsymbol{\chi}_s^{(2)} L(2\omega) L(\omega) L(\omega) : \mathbf{E}(\omega)\mathbf{E}(\omega)$ to be induced.[1] Here, $\boldsymbol{\chi}_s^{(2)}$ denotes the surface nonlinear susceptibility tensor with the components $\boldsymbol{\chi}_{s,\perp\perp\perp}^{(2)}$, $\boldsymbol{\chi}_{s,\perp\parallel\parallel}^{(2)}$, and $\boldsymbol{\chi}_{s,\parallel\perp\parallel}^{(2)}$. $L(\omega)$ and $L(2\omega)$ are the local-field correction factors for the pump and generated optical fields $\mathbf{E}(\omega)$ and $\mathbf{E}(2\omega)$, respectively. In addition, taking into account that in the presence of a propagating wave, planes perpendicular to $\mathbf{k}(\omega)$ are no longer mirror planes, the spatial derivative of the electric field gives rise to a longitudinal bulk (in leading order electric-quadrupole and magnetic-dipole) contribution to the SH-dipole moment $\mathbf{P}^{(2)}(2\omega) \propto \mathbf{E}(\omega) \nabla \mathbf{E}(\omega)$.[1,5] This results in a reflected SH wave originating from the bulk. Due to the boundary conditions, both source polarizations—local interfacial and bulk multipolar—are *a priori* indistinguishable for planar interfaces.[1,5]

The lack of an in-plane translational invariance for a single nanoscopic system, however, lifts the restriction of SH emission to particular directions. Here, as outlined in detail in (Refs. 7,8) in order to determine selection rules for emission from symmetry arguments, both the symmetry of the medium together with the experimental configuration represented by the wave vectors $\boldsymbol{k}(\omega)$ and $\boldsymbol{k}(2\omega)$ have to be considered. For centrosymmetric particles, due to cancellation of the transverse contributions of the *local* interface polarization the far-field SH response vanishes in the collinear forward and backward direction.[9] However, a *nonlocal* dipolar SH polarization could still arise from these distributed source terms due to propagation-induced phase lags between spatially separated points on the emitter. With this contribution oriented longitudinal, i.e., parallel to the quadrupolar bulk polarization, both source terms can only emit in noncollinear directions. Similarly, for the nanoscopic tip, in experimental configurations, which are sensitive only to the rotational symmetry, SHG is limited to these nonlocal longitudinal excitations. In addition, the lack of a mirror symmetry of the tip in the axial direction gives rise to a fully local surface dipole-allowed SH contribution. Thus by proper selection of observation direction and SH polarization these different contributions can be studied independently, providing information about the surface as well as bulk properties of the nanostructure.

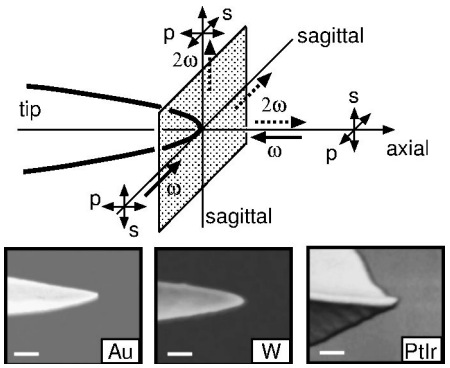

FIG. 1. Experimental geometry (top panel): Metal tips are illuminated in the axial or sagittal directions $\boldsymbol{k}(\omega)$ and scattered second-harmonic light $\boldsymbol{k}(2\omega)$ is detected for all symmetrically distinct configurations. Note that the definition of *s* or *p* polarization refers to the plane spanned by the respective wave vectors, and the tip axis, and may differ from common convections. Bottom panel: Electron micrographs of the different kinds of metal tips used for the experiments (scale bar: 100 nm). Due to the local field enhancement the SH response is confined to the near apex region (Ref. 17).

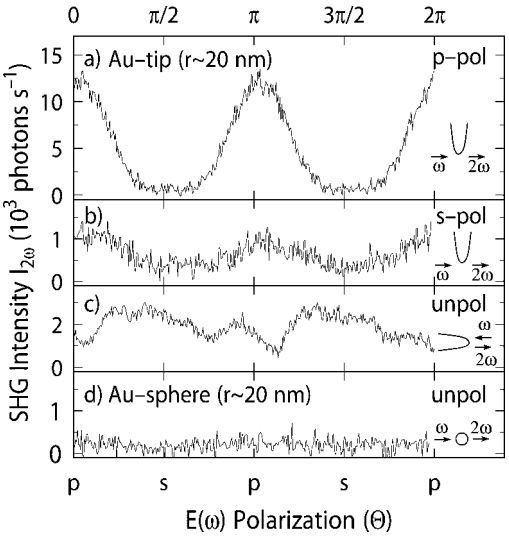

FIG. 2. Second-harmonic polarization dependence for a Au-tip with radius $r \sim 20$ nm. For sagittal pump illumination and collinear (a) *p*- and (b) *s*- polarized detection, SHG is dominated by the local dipole allowed $p_{\mathrm{in}}p_{\mathrm{out}}$ contribution. For axial excitation and collinear axial detection (c) SHG is forbidden (signal due to surface roughness). Similarly, for the case of small spherical Au nanoparticles, emission is not allowed in the exact forward and backward direction (d) (Refs. 3,4).

Except for specially designed arrangements[10] asymmetric nanosystems require investigation on the isolated particle level. In our experiments, a mode-locked Ti:sapphire oscillator was used (pulse duration <15 fs, center wavelength $\lambda = 805$ nm, repetition rate 72 MHz). The linearly polarized light is collimated onto the sharp end of a free standing tip by means of achromatic reflective optics. With a focus diameter of 12 μm exceeding by far the tip apex dimensions, plane wave excitation has been ensured—necessary in order to avoid SH contributions due to intensity gradients. Coarse directional information about the SH emission is obtained by limiting the detection angle to $\theta \leqslant 40^{\circ}$ (i.e., NA $\leqslant 0.35$). The second-harmonic light is spectrally selected with a dichroic filter and monochromator, and detected using a photomultiplier tube and photon counting electronics. It was verified that the signal was purely of second harmonic in nature up to the maximum experimental pump fluence of 40 GW cm^{-2}.

For the experiments, radially symmetric gold (Au) and tungsten (W) tips were obtained by electrochemical etching[11] with special emphasis paid to regular shape and smooth surface. Tip radii ranged from $\lesssim 10$ to 50 nm as characterized by electron microscopy. In addition, commercial pyramidal-shaped PtIr-coated atomic force microscopy tips were investigated. A representative set of the different tips used is shown in Fig. 1 (lower panel). Isolated spherical gold nanoparticles with nominally 40 nm diameter deposited on a glass slide, as well as flat surfaces of gold served as SH references.

A scheme of the experimental geometry is shown in Fig. 1 (upper panel). The tip is illuminated in the axial or sagittal direction and selected combinations of pump wave vector $\boldsymbol{k}(\omega)$ and observation directions $\boldsymbol{k}(2\omega)$ are investigated, which are symmetrically distinct and representative for the expected spatial and polarization emission characteristics. Figure 2 shows the dependence of the SH intensity on the input polarization for collinear sagittal illumination and SH detection, i.e, $\boldsymbol{k}(\omega) \| \boldsymbol{k}(2\omega)$, for a Au tip with radius $r \simeq 20$ nm. The signal is detected *p* (trace *a*) and *s* polarized (trace *b*) (for a definition of *p* and *s* polarization, see Fig. 1). In this configuration, the signal is dominated by the $p_{\mathrm{in}}p_{\mathrm{out}}$ polarization combination. The weak *s*-polarized contribution we attribute to the tip apex being slightly askew and/or rotationally asymmetric. The behavior is a direct manifestation of the broken symmetry of the tip along the axial direction, but is in marked contrast to the SH scattering for a spherical nanoparticle [as shown in Fig. 2(d)], where the overall inversion symmetry forbids SHG in a collinear geometry. Therefore this configuration probes exclusively the local surface dipolar SH polarization since the simultaneously induced nonlocal source polarizations are longitudinal and can only radiate in the noncollinear configuration as discussed below.

Under illumination of the tip in the axial direction, the SH signal is expected to vanish in the backwards direction due to the *mm* symmetry, as in the case of the sphere. In our experiment, however, the interaction of the pump with the entire shaft surface leads to a considerable background [Fig. 2(c)]. From rotating the tip around its axis and varying the illumination conditions we can attribute this signal to surface roughness and aforementioned symmetry imperfections with no discernible contribution from the tip apex. The emission of the nonlocal longitudinal bulk SH polarization induced along the tip axis in this illumination geometry, on the other hand, can be detected in the sagittal direction. In Figs. 3(a) and 3(b) data for both *p* and *s* SH polarization, respectively, are plotted. While *s*-polarized SH output remains forbidden both $p_{\mathrm{in}}p_{\mathrm{out}}$ and $s_{\mathrm{in}}p_{\mathrm{out}}$ are observed. Similar results are obtained for the $\mathrm{sagittal}_{\mathrm{in}}-\mathrm{axial}_{\mathrm{out}}$ combination (data not shown). In Figs. 3(c) and 3(d), results are shown for crossed $\mathrm{sagittal}_{\mathrm{in}}-\mathrm{sagittal}_{\mathrm{out}}$ configuration. Here, both the interfacial

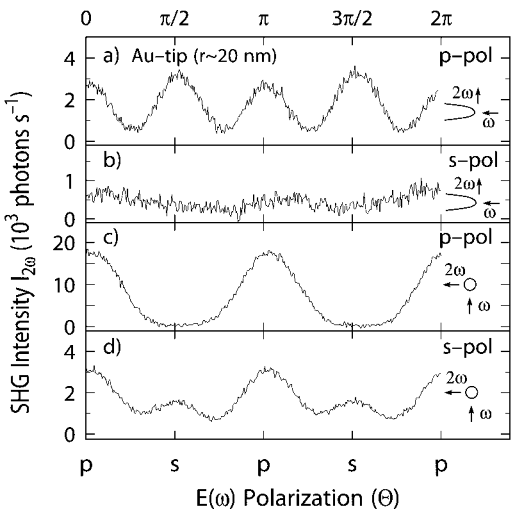

FIG. 3. Polarization dependence for axial illumination and sagittal (a) *p*- and (b) *s*-polarized SH detection. Similar to spherical particles only the nonlocal terms contribute to SHG. In contrast, both local *p*- (c) and nonlocal *s*-polarized contributions can be observed in the orthogonal $\text{sagittal}_{\text{in}}-\text{sagittal}_{\text{out}}$ configuration (d) Schematics: side (a), (b) and on axis (c), (d) view.

local dipole allowed $p_{\text{in}}p_{\text{out}}$ (trace *c*) as well as the nonlocal $p_{\text{in}}s_{\text{out}}$ and $s_{\text{in}}s_{\text{out}}$ polarization combinations (trace *d*) are observed. The polarization dependence for the local contribution exhibits a twofold periodicity, as expected [Fig. 3(c)]. The signal modulation observed in Fig. 3(d) for the nonlocal response we attribute to the interaction of distinct plasmon modes excited parallel or perpendicular to the tip axis.

For tungsten tips, the same behavior has been observed albeit at lower signal intensities. The signal levels from different tips of nominally similar radii are found to vary by less than a factor of two. In contrast, for the PtIr-coated uneven pyramidal (i.e., defying rotational symmetry) tips, only the strong local dipole contribution could be clearly identified (data not shown).

In the following we restrict the analysis to the high symmetry configurations as summarized in Table I. Here, the relative signal levels for different Au and W tips are qualitatively classified as *h*, *m*, and *w* representing high, intermediate and weak relative SH-signal strength (ratio of roughly 10:2:1). The data are juxtaposed with the symmetry selection rules that can be derived from the phenomenological description as outlined in the introduction. For each configuration, the possible mechanisms for nonlinear excitation followed by SH emission are indicated—specified *l* and *nl* for local and nonlocal. As in the case of planar surfaces the axial asymmetry permits a fully local dipolar SH response from the interface of the apex (termed $l \rightarrow l$ in the table). This is the dominating SH source from the metal tips in all $\text{sagittal}_{\text{in}}-\text{sagittal}_{\text{out}}$ $p_{\text{in}}p_{\text{out}}$ configurations and is due to the strong $\chi^{(2)}_{s,\perp\perp\perp}$ tensor element.[1] Judging from the weak $s_{\text{in}}p_{\text{out}}$ signal, contributions from $\chi^{(2)}_{s,\perp\|\|}$ can be neglected. Note that $\perp$ and $\|$ refer to the local coordinate system of the respective surface elements of the tip. For all other configurations SHG relies either on a nonlocal source polarization, e.g., bulk electric quadrupolar ($nl \rightarrow l$), or on the nonlocal coupling of

TABLE I. Directional and polarization symmetry selection rules for SHG scattering for asymmetric nanostructures. Relative signal intensities for the metal wire tips are qualitatively categorized as *h*, *m*, and *w* for high, intermediate and weak, respectively. The different local *l* and nonlocal *nl* excitation and emission mechanisms are indicated.

Detection(2ω)		Excitation(ω): sagittal		axial	
	pol	*s*	*p*	*s*	*p*
sagittal, collinear	*s*	**0**	(**w**) 0	–	–
sagittal, collinear	*p*	**0** $l^a \rightarrow l$	**h** $l \rightarrow l$	–	–
sagittal, orthogonal	*s*	**w** $l^a \rightarrow nl, nl \rightarrow l$	**m** $l^a \rightarrow nl, nl \rightarrow l$	**0**	**0**
sagittal, orthogonal	*p*	**0** $l^a \rightarrow l$	**h** $l \rightarrow l$	**w** $l^a \rightarrow l, nl \rightarrow l$	**w** $l^a \rightarrow l, nl \rightarrow l$
axial	*s*	**0**	**0**	**0**	**0**
axial	*p*	**w** $l^a \rightarrow nl, nl \rightarrow l$	**m** $l^a \rightarrow nl, nl \rightarrow l$	**0**	**0**

[a] By symmetry allowed ($\chi^{(2)}_{s,\perp\|\|}$), but not observed.

local interfacial SH polarizations ($l \rightarrow nl$). The longitudinal nature of these nonlocal source terms implies not only the absence of collinear SH emission in the axial direction but also the absence of *s*-polarized SH light for coplanar pump-detection geometries, i.e, $\boldsymbol{k}(2\omega)$ in plane with the tip axis and $\boldsymbol{k}(\omega)$. This is in accordance with our experimental results where corresponding signals were zero or small compared to SHG from any of the symmetry-allowed configurations.[12]

In the collinear $\text{sagittal}_{\text{in}}-\text{sagittal}_{\text{out}}$ configuration the selection rules are equivalent to that of a planar surface (dashed box in Table I). The response of configurations that are insensitive to the reduced symmetry resembles those of spherical or ellipsoidal particles (dotted boxes). Unique for the tip as a partially asymmetric nanostructure are configurations without any mirror plane (crossed $\text{sagittal}_{\text{in}}-\text{sagittal}_{\text{out}}$), where all polarization combinations can contribute to the SH response.[13] With the collinear sagittal measurements providing the pure surface tensor elements, this allows for the separation of the local interfacial and nonlocal bulk contributions. The *a priori* unknown and possibly complex angular distribution of the total SH signal does not allow for a straightforward quantitative comparison between local and nonlocal contributions.

The contribution of the local field-enhancement on SHG from the metal tips can be derived comparing the signal strength obtained with that of a planar surface of the same material. For the local interfacial emission, assuming a dipolar radiation distribution and approximating the effective tip area by an inscribed hemisphere with apex radius, this translates into a SH enhancement of $\sim 5 \times 10^3 - 4 \times 10^4$ for Au tips with $r \simeq 20$ nm. Assuming the SH power $\propto E^4$ this corresponds to an amplification of 8–14 for the average electric field near the apex. This value increases to $\lesssim 25$ for tips with a smaller radius of curvature in the 10-nm range and drops significantly as the tip radius increases. For both W and PtIr significantly lower values for the SH enhancement are found corresponding to local field factors between 3 and 6. These values derived for the local field enhancement are consistent

with observations from tip-enhanced Raman spectroscopy.[14]

A simple model can be applied to estimate the local-field enhancement treating the tip as a hemispheroid.[15] In the electrostatic limit the local-field correction factor for the plane wave component perpendicular to the apex is given by $L_\perp \simeq \varepsilon_m\{\varepsilon+(\varepsilon_m-\varepsilon)A\}^{-1}$ with ε_m and ε the dielectric constants of metal and surrounding, respectively, and A the depolarization factor, a function of the aspect ratio. With values for the aspect ratio in the range of 2 to 6 derived from electron microscopy and the dielectric functions for Au ($\varepsilon_m=-26.8+1.88i$) and W ($\varepsilon_m=5.0+19.4i$) (Ref. 16) at $\lambda=805$ nm, $L_\perp(\omega)$ would range from 5 to 14 for W and 7 to 120 for Au, with the latter enhancement due to plasmon resonance contributions. Taking the average of $L_\perp(\omega)$ across the curved apex area the results fall within the range of the experimentally observed values.

With the selection rules being generally applicable to partially asymmetric nanostructures, this allows for the simultaneous investigations of surface and bulk properties on the nanoscale. This can provide more detailed information in studies of, e.g., SHG from metallic tips for the purpose of scattering-type near-field microscopy[17] and SHG from nanostructured or percolated metal island films[18] or from colloidal particles.[4,19]

Note added in proof. The linear light scattering of nanoscopic metal tips in terms of spectral and polarization dependence of the emission has been investigated in Ref. 20.

We gratefully acknowledge invaluable support from Th. Elsaesser and K. Reimann and helpful discussions with M. Fiebig, T. F. Heinz and A. J. Yodh.

[1] T. F. Heinz, in *Nonlinear Surface Electromagnetic Phenomena*, edited by H.-E. Ponath and G. I. Stegeman (North-Holland, Amsterdam, 1991), p. 353.

[2] Y. R. Shen, in *Frontiers in Laser Spectroscopy*, edited by T. W. Hänsch and M. Inguscio (North-Holland, Amsterdam, 1994), p. 139; *Nonlinear Optics at Interfaces*, edited by E. Matthias and F. Träger, special issue of Appl. Phys. B 210 (3), (1999).

[3] J. I. Dadap, J. Shan, K. B. Eisenthal, and T. F. Heinz, Phys. Rev. Lett. **83**, 4045 (1999); J. I. Dadap, J. Shan, and T. F. Heinz, J. Opt. Soc. Am. B **21**, 1328 (2004).

[4] N. Yang, W. E. Angerer, and A. G. Yodh, Phys. Rev. Lett. **87**, 103902 (2001); V. L. Brudny, B. S. Mendoza, and W. L. Mochán, Phys. Rev. B **62**, 11152 (2000).

[5] B. Koopmans, F. van der Woude, and G. A. Sawatzky, Phys. Rev. B **46**, 12780 (1992); J. E. Sipe, V. Mizrahi, and G. I. Stegeman, *ibid.* **35**, 9091 (1987).

[6] E. C. Hao, G. C. Schatz, R. C. Johnson, and J. T. Hupp, J. Chem. Phys. **117**, 5963 (2002).

[7] S. Roke, M. Bonn, and A. V. Petukhov, Phys. Rev. B **70**, 115106 (2004); A. V. Petukhov, V. L. Brudny, W. L. Mochán, J. A. Maytorena, B. S. Mendoza, and Th. Rasing, Phys. Rev. Lett. **81**, 566 (1998).

[8] T. F. Heinz and D. P. DiVincenzo, Phys. Rev. A **42**, 6249 (1990).

[9] In general, with both incoming and outgoing wave vectors lying within one, and the same mirror plane of a *mm*-symmetric structure, then no net signal polarized normal to this plane can be radiated since for each point on the surface emitting such a radiation there exists a mirror point producing the same and opposite contribution that leads to cancellation of the farfield.

[10] B. Lamprecht, A. Leitner, and F. R. Aussenegg, Appl. Phys. B **68**, 419 (1999).

[11] J. P. Ibe *et al.*, J. Vac. Sci. Technol. A **8**, 3570 (1990).

[12] It should be noted that the selection rules derived are strictly valid only in the Rayleigh limit for sufficiently small tip apex dimensions, which implies a collective (linear and/or nonlinear) excitation: a natural prerequisite for the validity of our model.

[13] In sum-frequency generation (SFG) with two independent input beams, additional degrees of freedom exist to built asymmetric configurations; see: S. Roke *et al.*, Phys. Rev. Lett. **91**, 258302 (2004).

[14] A. Hartschuh, E. J. Sánchez, X. S. Xie, and L. Novotny, Phys. Rev. Lett. **90**, 095503 (2003).

[15] C. K. Chen, T. F. Heinz, D. Ricard, and Y. R. Shen, Phys. Rev. B **27**, 1965 (1983).

[16] *Handbook of Optical Constants of Solids*, edited by E. D. Palik (Academic Press, San Diego, 1985).

[17] A. Bouhelier, M. Beversluis, A. Hartschuh, and L. Novotny, Phys. Rev. Lett. **90**, 013903 (2003); M. Labardi *et al.*, Opt. Lett. **29**, 62 (2004); S. Takahashi and A. V. Zayats, Appl. Phys. Lett. **80**, 3479 (2002).

[18] M. I. Stockman, D. J. Bergman, C. Anceau, S. Brasselet, and J. Zyss, Phys. Rev. Lett. **92**, 057402 (2004); S. I. Bozhevolnyi, J. Beermann, and V. Coello, *ibid.* **90**, 197403 (2003); A. V. Zayats, T. Kalkbrenner, V. Sandoghdar, and J. Mlynek, Phys. Rev. B **61**, 4545 (2000).

[19] H. Wang, E. C. Y. Yan, E. Borguet, and K. B. Eisenthal, Chem. Phys. Lett. **259**, 15 (1996).

[20] C. C. Neacsu, G. A. Steudle, and M. B. Raschke, Appl. Phys. B **80**, 295 (2005).